Equivalent Circuit-Based Simulation of Half-Car Piezoelectric Energy Harvesting on Degraded Urban Road Profiles

Nadia El atlas[1,*] and *Abdelmajid* Bybi[1,**]

[1]Mohammed V University in Rabat, Higher School of Technology of Salé, MEAT - Materials Energy and Acoustics Team, Avenue Le Prince Héritier, B.P 227, 11000 Salé Médina, Morocco

Abstract. This study compares three excitation modeling approaches—deterministic mixed scenarios, Gaussian stochastic models, and AR(1) stochastic models—to evaluate the energy harvesting potential of a half-car suspension system equipped with front and rear piezoelectric stack harvesters. The half-car suspension is modeled using equivalent electrical circuits based on the force-voltage analogy. Each excitation model is implemented and simulated in MATLAB/Simulink to analyze and compare the harvested energy under varying road profiles. This work highlights the influence of excitation modeling on the accuracy and realism of energy recovery assessments in vehicular suspension systems.

1 Introduction

Vibration-based energy harvesting in vehicles has gained increasing attention as a means of powering low-consumption electronic systems without relying on external energy sources[1]. Piezoelectric harvesters integrated into suspension systems offer a compact and efficient solution for converting mechanical vibrations induced by road irregularities into electrical energy [2]. However, the accuracy of such energy assessments depends heavily on how the road excitations are modeled, as they directly influence the dynamic response of the suspension system. Recent studies have explored energy harvesting from vehicle suspensions, focusing on the impact of road roughness and driving conditions. Zhao et al. [3] developed a piezoelectric energy harvester using noncontact magnetic force, achieving up to 24.28 W on random roads and 3346 W on pulse roads. Abdelkareem et al. [4] investigated a double-sided arm-toothed electromagnetic harvester for semi-trailer trucks, generating 0.33–21.3 W across various road classes. Benhiba et al. [5] simulated piezoelectric energy harvesting from passive car suspensions under random excitations, while Hu et al. [6] examined galloping piezoelectric energy harvesters in low-velocity water flow, considering surface roughness effects. These studies demonstrate that road roughness significantly influences harvested power, with higher roughness generally yielding more energy. Additionally, factors such as driving speed, vehicle load, and harvester design play crucial roles in determining energy output [7].

Many existing studies rely on deterministic excitations—such as idealized bumps, potholes, or profile scenarios—[3, 8, 9] which provide reproducible inputs for targeted analysis and experimental validation [10]. Yet, these inputs are limited in their ability to reflect the

*e-mail: nadia.elatlas@research.emi.ac.ma
**e-mail: abdelmajid.bybi@est.um5.ac.ma

randomness and spectral variability of real road surfaces. To address this, stochastic models, particularly those based on Gaussian processes, have been widely adopted and standardized in the literature [11–13]. Xu et al. [12] proposed an amplitude modulation method to synthesize non-Gaussian road profiles with controllable kurtosis, demonstrating increased fatigue damage potential with higher kurtosis. Ma et al. [13] developed a harmonic superposition method to generate random road excitation signals for different vehicle speeds and road classifications. Bogsjö et al. [11] introduced three new road profile models, including Laplace and hybrid Gaussian–Laplace processes, which showed improved accuracy compared to classical Gaussian models when fitted to measured road surfaces. Zhan-zong [3] presented a time-domain excitation model for left and right wheel tracks using inverse fast Fourier transform, considering the coherence between tracks. Non-stationary vehicle vibrations can be decomposed into Gaussian elements, revealing that magnitude variations cause the non-Gaussian nature of the process [14]. ARIMA models have been used to characterize non-stationary road profiles, with recent developments suggesting the use of random variables for autoregressive coefficients to introduce uncertainty and generate terrain topology distributions [15]. These approaches aim to improve the accuracy of road excitation modeling, which is essential for vehicle design, fatigue assessment, and structural health monitoring and energy harvesting evaluation. The complexity and variability of road-related vibrations underscore the need for sophisticated analysis and synthesis methods in the field.

Despite the importance of excitation modeling, few works have systematically compared the impact of deterministic and stochastic road profiles on the energy harvesting potential of suspension systems[10, 16]. This study aims to fill this gap by conducting a comparative simulation study using a half-car model equipped with front and rear piezoelectric stack harvesters. The system is modeled using equivalent electrical circuits based on the force-voltage analogy[5, 17, 18], a technique that enables straightforward integration into simulation platforms such as MATLAB/Simulink. The objective is to quantify how the choice of excitation model influences the harvested energy and to provide guidelines for selecting road models in future energy harvesting studies and design processes.

This paper is structured as follows. Section 2 introduces the half-car model with piezoelectric stack harvesters. Section 3 presents its equivalent electrical circuit. Section 4 describes the road excitation models: deterministic, ISO 8608 Class H, and AR(1). Section 5 discusses the simulation results and harvested power, and Section 6 concludes the study.

2 Half-Car Model with Piezoelectric Stack Harvesters

The proposed half-car model (HCM) is a four-degree-of-freedom (4-DOF) system that accounts for both vertical translation and pitch rotation of the vehicle body. It comprises a sprung mass m_s and two unsprung masses m_{uf} and m_{ur} representing the front and rear wheels, respectively. The suspension systems are modeled as spring-damper pairs: (k_{sf}, b_{sf}) for the front and (k_{sr}, b_{sr}) for the rear. The tire dynamics are represented by additional spring-damper pairs: (k_{uf}, b_{uf}) and (k_{ur}, b_{ur}).

To enable vibration-based energy recovery, a piezoelectric stack transducer is integrated in series with each suspension unit at the front and rear axles. The road excitations z_{rf} and z_{rr} are applied independently beneath the front and rear wheels. This configuration allows the model to capture the coupled dynamics of vertical motion and pitch, while enabling the assessment of energy harvesting performance at both axles under realistic degraded road profile.

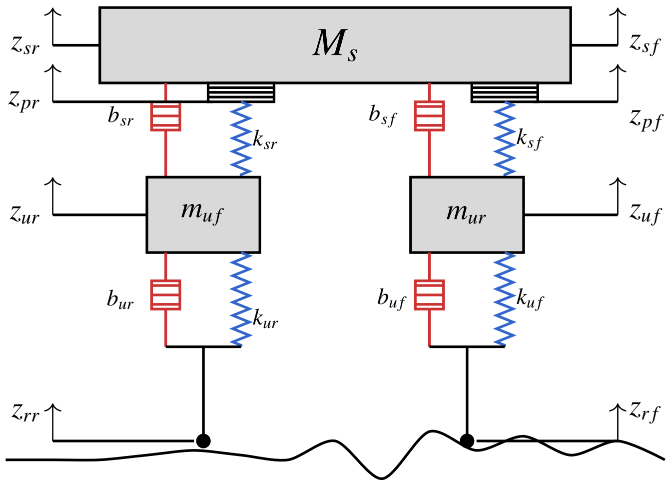

Figure 1: Half-car model with front and rear piezoelectric stack harvesters under a degraded urban road profile.

3 Equivalent Circuit of the HCM

The electrical equivalent circuit of the half-car model is derived using the force–voltage analogy (see Table 1), in which mechanical force corresponds to voltage and velocity to current. This analogy enables the mapping of masses, dampers, and springs to inductors, resistors, and inverse capacitors, respectively. The resulting topology has been validated in one of our recent studies without the energy harvesting integration[18]. In the present work, a simplified Mason equivalent circuit 2, representing a multilayer piezoelectric stack harvester, is inserted in parallel with the suspension branch analogous to the spring at both the front and rear suspensions. Figure 2 illustrates the structure of the simplified Mason circuit, which consists of a mechanical port modeled by a source F_p in series with C_p, L_p, and R_p, a transformer with turns ratio $N : 1$, and an electrical port comprising the clamped capacitance C_0 and a resistive load R_{load}. The complete electrical equivalent of the half-car system with front and rear energy harvesters is shown in Figure 3.

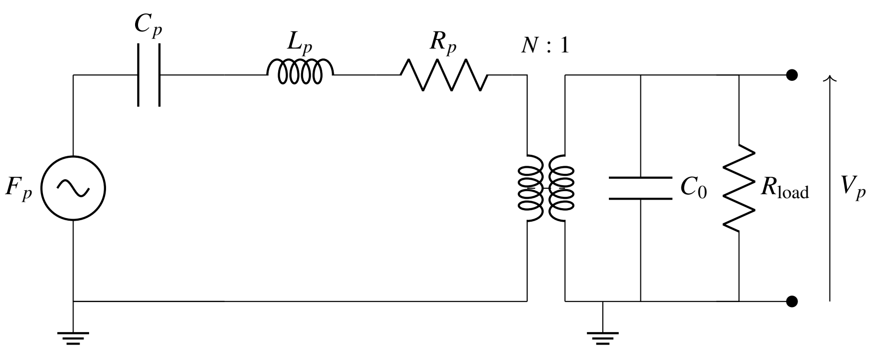

Figure 2: Simplified Mason circuit for multilayer PZT energy harvester.

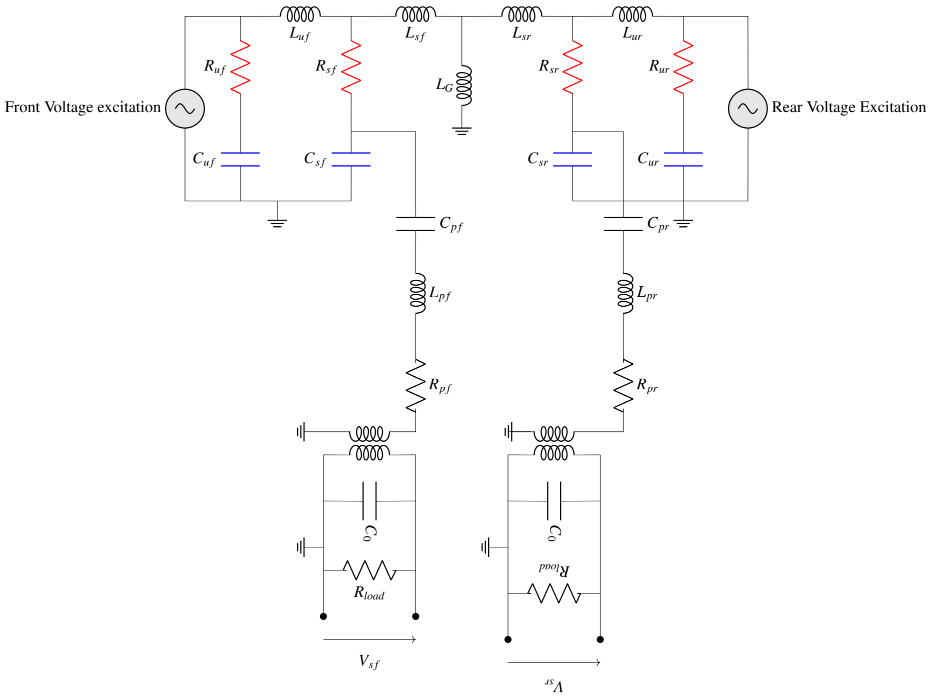

Figure 3: Electrical equivalent circuit of half-car suspension system with front and rear piezoelectric energy harvesters.

Table 1: Electromechanical analogy (force–voltage).

Mechanical	Electrical	Unit
F	V	N / V
$\dot{x}$	i	m/s / A
m	L	kg / H
b	R	N·s/m / Ω
k	$1/C$	N/m / 1/F
x	q	m / C

4 Road Excitation Modeling for Urban Degraded Road

To investigate the impact of road surface variability on energy harvesting performance, three types of vertical excitations were considered: a deterministic urban scenario, a stochastic profile based on ISO 8608 (Class H), and an autoregressive AR(1) signal with equivalent RMS acceleration.

For all cases, the simulation duration was set to $T = 12\,\text{s}$, with a sampling frequency of $f_s = 1000\,\text{Hz}$. The vehicle velocity was fixed at $V = 30\,\text{km/h}$, and the wheelbase was $L = 2.88\,\text{m}$, resulting in a time delay $\tau = L/V \approx 0.3456\,\text{s}$ between front and rear wheel excitations.

4.1 Deterministic Urban Road Scenario

The first excitation (Figure 4) corresponds to a synthetic yet realistic urban driving sequence. The front wheel displacement was constructed by concatenating four consecutive road segments:

- A smooth section from 0 to 4 s, characterized by low-amplitude undulations representing regular asphalt.
- A rough section from 4 to 9 s, modeled using a high-frequency stochastic AR(1) process to realistically capture the correlated irregularities of degraded pavement.
- A localized speed bump between 9 and 10 s, represented as a deterministic elevation to simulate traffic calming devices.
- A pothole segment from 10 to 12 s, modeled as a sudden surface depression.

This composite profile combines deterministic and stochastic components, enabling a comprehensive evaluation of energy harvesting performance under realistic and variable urban road conditions. The rear excitation was obtained by applying a time delay τ to the front wheel signal.

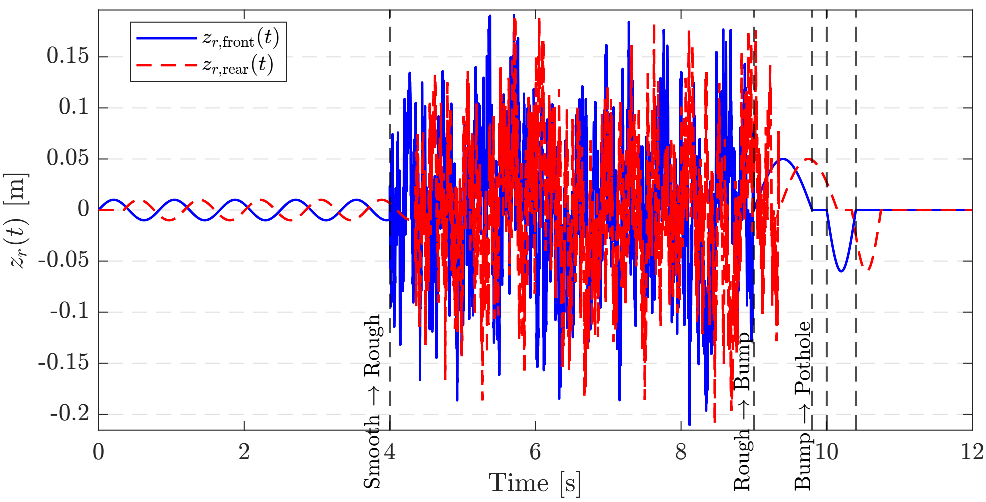

Figure 4: Urban road profile scenario used in the half-car energy harvesting simulation. The signal includes four consecutive segments: Smooth (0–4 s), Rough (4–9 s), Speed Bump (9–10 s), and Pothole (10–12 s).

4.2 ISO 8608 Class H Road Profile

The second excitation (Figure 5) was generated according to ISO 8608 specifications for road roughness. The vertical displacement is modeled as a spatially stationary Gaussian process, with the spatial power spectral density (PSD) given by:

$$G_q(n) = G_q(n_0)\left(\frac{n}{n_0}\right)^{-w}$$

where $G_q(n_0) = 1024 \times 10^{-6}\,\mathrm{m^3/cycle}$ corresponds to Class H roughness, $n_0 = 0.1\,\mathrm{cycle/m}$ is the reference spatial frequency, and $w = 2$ is the spectral slope. The PSD was sampled in the frequency domain and converted into the time domain using the inverse

Fourier transform, scaled by the vehicle velocity. The rear signal was obtained via the same time delay τ.

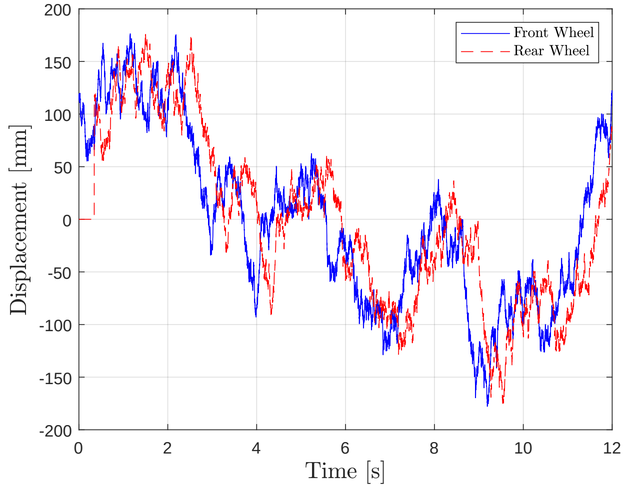

Figure 5: Front and rear road excitations generated from a Gaussian stochastic process using MATLAB.

4.3 AR(1) Profile

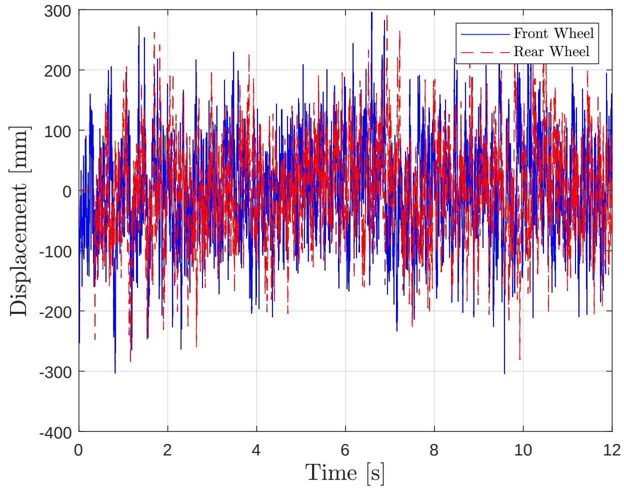

Figure 6: Front and rear road excitations generated from an AR(1) stochastic process using MATLAB.

To capture the effects of temporal correlation, a third excitation was generated using a first-order autoregressive process:

$$z_k = \alpha z_{k-1} + \beta \eta_k$$

with α = 0.95 and η_k being standard Gaussian white noise. The coefficient β was calibrated to match the RMS amplitude of the ISO-based profile, ensuring equal energy content. Compared to the Gaussian excitation, the AR(1) signal contains longer correlation lengths and smoother transitions, which can lead to more intense excitation bursts. The rear signal was again obtained by time-shifting the front profile by τ. This modeling framework enables a comprehensive comparison of the voltage response under deterministic and stochastic excitations representative of degraded urban road conditions. The corresponding front and rear wheel displacement signals are illustrated in Figure 6.

5 Results and Discussion

The half-car model equipped with piezoelectric harvesters was subjected to three types of vertical road excitations: a deterministic mixed scenario, and two stochastic signals (Gaussian and AR(1)-based). The simulations were performed over 12 s, corresponding to a vehicle speed of 30 km/h. Both front and rear suspensions were equipped with multilayer piezoelectric stacks, placed in parallel with the suspension springs.

5.1 Voltage and Power Recovery

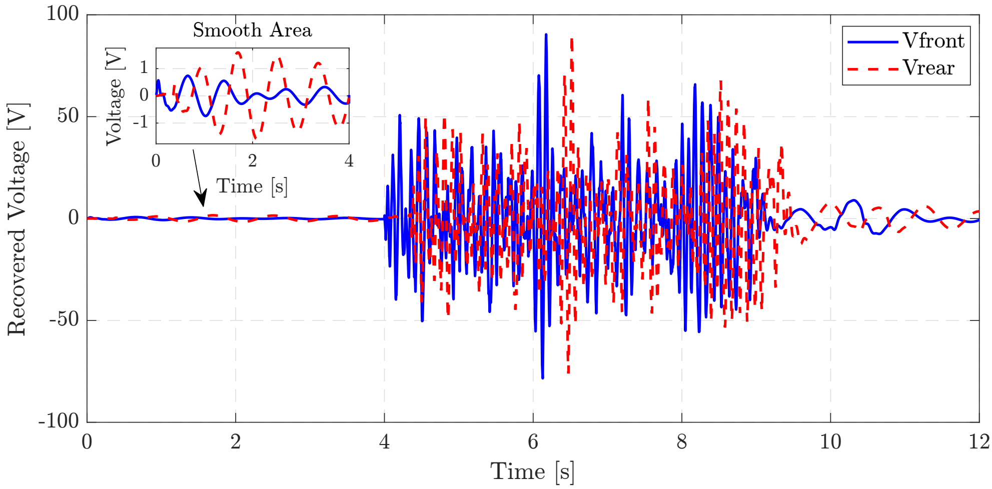

Figure 7: Recovered voltage from the mixed scenario excitation. Both front and rear piezoelectric harvesters show similar voltage profiles, with higher peaks during the rough and bump phases.

For the deterministic scenario-based excitation, the results (Figure 7, Figure 8 and Table 2) show that the majority of the recovered energy originates from the rough phase, with approximately 2.98 J at the front and 2.86 J at the rear, accounting for nearly the entire harvested energy during the simulation. The bump phase yields significantly more energy at the rear (0.22 J) than at the front (0.019 J), likely due to the delayed excitation and increased dynamic amplification at the rear axle resulting from the vehicle's pitch motion and suspension characteristics. As expected, the smooth phase contributes minimally, given the limited surface excitation. The pothole phase generates a small amount of energy, slightly higher at the front than at the rear, likely due to the more abrupt initial impact experienced by the front wheel and the partial damping of this disturbance before it reaches the rear suspension. The RMS values of voltage and power indicate a generally symmetric performance between front and rear harvesters, with RMS power around 1 W.

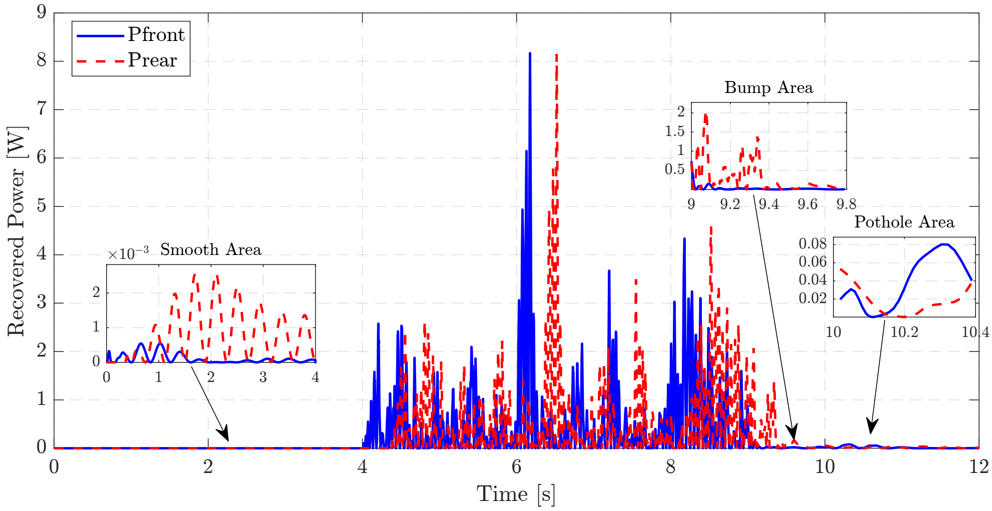

Figure 8: Recovered voltages from piezoelectric harvesters: front and rear excitations.

Table 2: Recovered energy (J) and RMS values for front and rear piezoelectric harvesters

Phase	Front Energy (J)	Rear Energy (J)
Smooth	0.00041	0.00310
Rough	2.97745	2.85689
Bump	0.01897	0.21909
Pothole	0.01471	0.00620
Total	**3.03217**	**3.11709**

Quantity	Front	Rear
RMS Voltage (V)	23.45	23.36
RMS Power (W)	1.02	1.00

Table 3: Quantitative comparison of harvested power and energy for AR(1) and Gaussian models

Model	Wheel	Mean Power (W)	Max Power (W)	Total Energy (J)
AR(1)	Front	0.0943	1.4690	1.1379
AR(1)	Rear	0.0909	1.5116	1.1118
Gaussian	Front	0.0022	0.0279	0.0259
Gaussian	Rear	0.0027	0.0849	0.0325

Figures 9 and 10, along with Table 3, provide a comprehensive comparison of the performance of the piezoelectric energy harvesting system mounted on a half-car model subjected

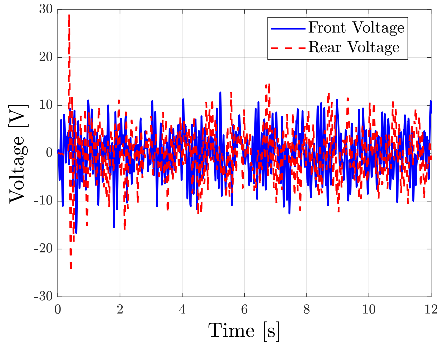

(a) Gaussian excitation (Class H urban road).

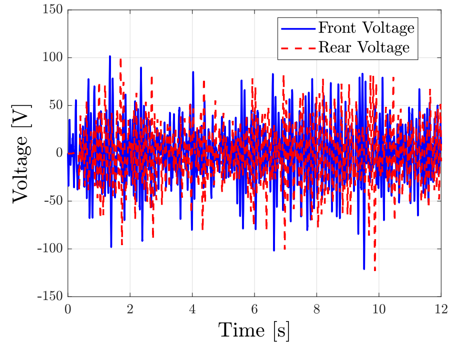

(b) AR(1) excitation with equivalent RMS acceleration.

Figure 9: Recovered voltage signals from front and rear harvesters under two different stochastic road profiles.

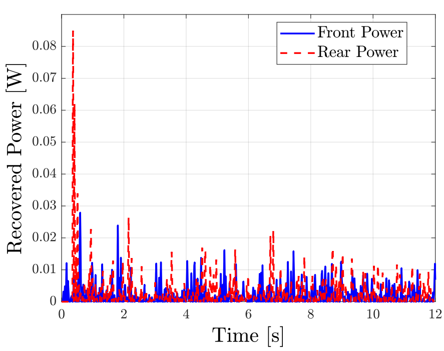

(a) Gaussian excitation (Class H).

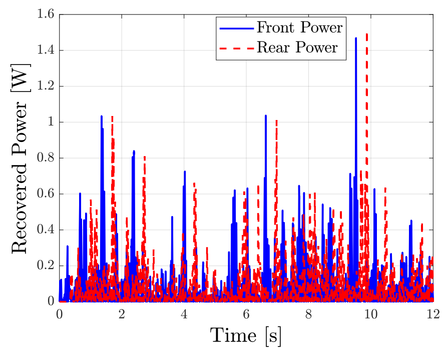

(b) AR(1) excitation with equivalent RMS acceleration.

Figure 10: Comparison of recovered power for two stochastic road excitations.

to two types of stochastic road excitations: Class H Gaussian excitation, representing a highly degraded urban road, and an AR(1) excitation with equivalent RMS acceleration. As shown in Figures 9a and 10a, the Gaussian excitation induces frequent voltage oscillations with moderate amplitude, resulting in low but continuous power recovery. In contrast, the AR(1) excitation (Figures 9b and 10b) produces sparser yet higher amplitude voltage and power peaks, indicating strong but intermittent mechanical excitations. This difference reflects the temporal correlation in the AR(1) input signal, which leads to more pronounced but less frequent dynamic responses.

Table 3 quantifies these findings by reporting the mean power, maximum power, and total harvested energy for each case. Under AR(1) excitation, the mean power reaches approximately 0.09 W, and the total harvested energy exceeds 1.1 J, confirming the superior energy harvesting capability of this input. Maximum power values also surpass 1.46 W for both front and rear harvesters.

In comparison, the Gaussian excitation yields much lower mean power values (less than 3 mW) and a lower total harvested energy (below 0.04 J).

The results highlight the importance of using stochastic excitations, such as AR(1) or Class H Gaussian profiles, when evaluating piezoelectric energy harvesters under realistic road conditions. While deterministic inputs are helpful for understanding instantaneous system responses, they are not suitable for assessing global performance.

Table 3 clearly shows that the AR(1) excitation yields the highest harvested energy and mean power, making it a better candidate for optimization and system design aimed at energy recovery from urban road vibrations.

6 Conclusion

This study highlights the important role of excitation modeling in accurately evaluating vibration-based energy harvesting systems for vehicles. The results show that the characteristics of road excitation greatly affect the amount of electrical energy harvested, especially when the suspension's dynamic response is controlled by resonance effects. Deterministic scenarios provide a controlled and repeatable way to analyze the system but do not capture the natural variability of real roads. Gaussian stochastic excitations are commonly used and standardized but tend to under-excite the system because of their broad frequency content. On the other hand, AR(1) excitations, when properly set, offer a more realistic approach by focusing energy around the vehicle's natural frequencies, which improves energy harvesting performance.

Based on these findings, a combined approach is recommended: use deterministic excitations for validation and AR(1)-based stochastic signals for more realistic performance evaluation. Although Gaussian models are useful for standard benchmarks, they should not be the only method for predictive analysis. In the future, including real road profile data into half-car simulation models would improve the accuracy and relevance of energy harvesting predictions under actual driving conditions.

References

[1] K. Nguyen-Vinh, N. Nguyen-Quang, H. Dewasurendra, A review of Low-Power energy harvesting technologies in industry 4.0, in *2023 5th International Conference on Electrical, Control and Instrumentation Engineering (ICECIE)* (IEEE, 2023), pp. 1–6

[2] H. Mastouri, A. Ennawaoui, M. Remaidi, E. Sabani, M. Derraz, H. El Hadraoui, C. Ennawaoui, Design, modeling, and experimental validation of a hybrid piezoelectric–magnetoelectric energy-harvesting system for vehicle suspensions, World Electric Vehicle Journal **16**, 237 (2025).

[3] Z. Zhao, B. Zhang, Y. Li, C. Bao, T. Wang, A novel piezoelectric energy harvester of noncontact magnetic force for a vehicle suspension system, Energy Science & Engineering **11**, 1133 (2023).

[4] M.A. Abdelkareem, R. Zhang, X. Jing, X. Wang, M.K.A. Ali, Characterization and implementation of a double-sided arm-toothed indirect-drive rotary electromagnetic energy-harvesting shock absorber in a full semi-trailer truck suspension platform, Energy **239**, 121976 (2022).

[5] A. Benhiba, A. Bybi, R. Alla, H. Drissi, E.A. Chater, M. Nabti, Modeling and simulation of vibrational energy harvesting from passive car suspension subjected to random excitations, in *2022 2nd International Conference on Innovative Research in Applied Science, Engineering and Technology (IRASET)* (IEEE, 2022), pp. 1–9

[6] S. Hu, D. Zhao, W. Sun, Y. Liu, C. Ma, Investigation on galloping piezoelectric energy harvester considering the surface roughness in low velocity water flow, Energy **262**, 125478 (2023).

[7] Y. Cao, J. Li, A. Sha, Z. Liu, F. Zhang, X. Li, A power-intensive piezoelectric energy harvester with efficient load utilization for road energy collection: Design, testing, and application, Journal of Cleaner Production **369**, 133287 (2022).

[8] L. Wang, P. Todaria, A. Pandey, J. O'Connor, B. Chernow, L. Zuo, An electromagnetic speed bump energy harvester and its interactions with vehicles, IEEE/ASME Transactions on Mechatronics **21**, 1985 (2016).

[9] P. Todaria, L. Wang, A. Pandey, J. O'Connor, D. McAvoy, T. Harrigan, B. Chernow, L. Zuo, Design, modeling and test of a novel speed bump energy harvester, in *Sensors and Smart Structures Technologies for Civil, Mechanical, and Aerospace Systems 2015* (SPIE, 2015), Vol. 9435, pp. 38–51

[10] R.C. Sharma, S. Palli, L.G. Rao, A. Duppala, S.K. Sharma, Four-wheel vehicle response under bump, pothole, harmonic, and random excitations using bond graph/simulink technique, SAE International Journal of Commercial Vehicles **16**, 129 (2022).

[11] K. Bogsjö, K. Podgórski, I. Rychlik, Models for road surface roughness, Vehicle System Dynamics **50**, 725 (2012).

[12] F. Xu, H. Yang, K. Ahlin, On vehicle response under non-gaussian road profile excitation, Advances in Mechanical Engineering **16**, 16878132241241676 (2024).

[13] K. Ma, Y. Zhang, X. Zhen, Simulation of pavement random excitation based on harmonic superposition method, International Journal of Scientific Advances **2**, 282 (2021).

[14] V. Rouillard, Statistical models for nonstationary and non-gaussian road vehicle vibrations., Engineering letters **17** (2009).

[15] S.M. Wagner, J.B. Ferris, A Polynomial Chaos Approach to ARIMA Modeling and Terrain Characterization, in *Proceedings of SPIE – The International Society for Optical Engineering, Smart Structures and Materials 2007: Sensors and Smart Structures Technologies for Civil, Mechanical, and Aerospace Systems* (SPIE, San Diego, CA, USA, 2007), Vol. 6564 of *SPIE Conference Series*, p. 65640D

[16] H. Guo, W. Zeng, D. Egloff, F. Meng, O. Dahlsten, Potential power output from vehicle suspension energy harvesting given bumpy and random-surfaced roads, Sustainability **16**, 6964 (2024).

[17] A. Benhiba, A. Bybi, H. Drissi, A. Salbi, O. Mouhat, I. Lahlouh, Equivalent circuits for vibrations' energy harvesting from automotive suspensions: Mason and martin models, Journal of Vibration Engineering & Technologies **13**, 171 (2025).

[18] N. El Atlas, A. Bybi, Simplified Modeling of Quarter and Half Car Suspension Systems Using Electrical Circuit Analogies, in *2025 5th International Conference on Innovative Research in Applied Science, Engineering and Technology (IRASET)* (IEEE, 2025), pp. 1–6